Original Research Articles

Histology to MRI registration quality of ex vivo human brain blocks fixed with solutions used in anatomy laboratories

Eve-Marie Frigon, Ph.D.[1][a], Amy Gérin-Lajoie, B.Sc.[1], Jérémie P. Fouquet, Ph.D.[2,3], Yashar Zeighami, Ph.D.[2,4], Denis Boire, Ph.D.[5], Mahsa Dadar, Ph.D.[2,4], Josefina Maranzano, MD., Ph.D.[1,6]

[1] Department of Anatomy, University of Quebec at Trois-Rivieres, Quebec, Canada, [2] Cerebral Imaging Centre, Douglas Mental Health University Institute, Quebec, Canada, [3] CHUS research Center, University of Sherbrooke, Quebec, Canada, [4] Department of Psychiatry, McGill University, Quebec, Canada, [5] Department of Anatomy, University of Qxuebec at Trois-Rivieres, Quebec, Canada, [6] Department of Neurology and Neurosurgery, McGill University, Quebec, Canada

Post-mortem brain tissue is obtained from brain banks that provide small samples that are fixed with neutral-buffered formalin (NBF), while gross anatomy laboratories could become a source of complete brains for neuroscientists. These are preserved with solutions developed for dissection, such as a saturated-salt-solution (SSS) or an alcohol-formaldehyde solution (AFS). Histology remains the gold standard in neuroscientific research, while MRI is the most common imaging modality. Thus, MRI-histology registration quality needs to be assessed in human brains fixed with NBF, SSS and AFS. To this end, we used 12 human brain blocks fixed in our anatomy laboratory (SSS=4; AFS=4; NBF=4). The blocks were scanned using a 7T Bruker animal MRI scanner with a T2-TurboRARE sequence and cut into 40μm sections, which were stained with histochemistry and immunohistochemistry. Stained sections were imaged using a slide scanner microscope and segmented with masks using Display, and the sections were manually registered to the T2-TurboRare images using landmarks in Register (MINCToolKit). Our results showed that more landmarks were needed to achieve proper alignment of the histology to MRI images for the SSS-fixed blocks. These blocks also showed a lower percentage of overlap between the good histology quality masks and the MRI masks. We conclude that our MRI and registration protocols are suitable for brains fixed with solutions used in gross anatomy laboratories, although more challenging when fixed with SSS. These results are promising for neuroscientists interested in using full brains from anatomy laboratories, either using MRI, histology or registration of both modalities to study normal aging and neurodegenerative conditions.

Magnetic resonance imaging (MRI) is the most common neuroimaging modality in neuroscientific research, since it is non-invasive and can provide good contrast between cortical gray matter (GMc) and white matter (WM), enabling assessment and quantification of different brain structures and pathologies. Different MRI acquisition protocols and technologies have been developed in the last few decades, increasing our ability to estimate whole brain, GMc and WM volumes,[1] volumetric and relaxation changes of specific structures in neurodegenerative diseases (e.g., hippocampal volume changes in dementia),[2,3] and lesion occurrence and their longitudinal evolution (e.g., WM hyperintensities in cerebrovascular disease).[4] However, to confirm MRI findings, histology remains the gold standard in neuroscientific research since it provides cellular resolution.[5,6] Being able to correlate MRI imaging with cellular histology is of utmost importance to establish a meaningful anatomical and pathophysiological conclusion.

Biopsies from living individuals for histopathological study can only provide very small samples and are rarely performed due to their invasive nature. Therefore, researchers commonly use post-mortem tissue samples that are generally provided by brain banks. However, brain banks usually provide limited numbers of small tissue samples, one hemisphere being fixed by immersion in neutral-buffered formalin (NBF), and the other frozen.[7,8] Alternatively, neuroscientists could obtain higher numbers of full brains from gross anatomy laboratories that collaborate

---

a Corresponding Author:
Eve-Marie Frigon
eve-marie.frigon@uqtr.ca

with body donation programs. These brains are fixed through whole-body perfusion, using solutions other than NBF, which are typically used in brain banks since the body is used for teaching gross anatomy. Our team's previous work has shown that two solutions used in our human anatomy laboratory, a saturated-salt solution (SSS) and an alcohol-formaldehyde solution (AFS), preserve antigenicity of the four main cell populations in mice brains[9] and in human brain samples.[10] This work established that histology of human brain tissue fixed with SSS or AFS is of sufficient quality for neuroscientific research, potentially increasing the amount of brain tissue available to neuroscientists for histological studies. Furthermore, performing MRI scans in these brains is also feasible, enabling correlations with histology findings.[11,12]

Since MRI is the most common neuroimaging modality, and histology remains the gold standard, registration of images obtained with these two modalities is essential to correlate findings.[13-15] Previous work on Alzheimer's disease,[16-21] Parkinson's disease,[22] strokes,[23] cerebrovascular diseases,[24-27] white matter hyperintensities,[28,29] multiple sclerosis,[30-33] etc., have used registration between MRI and histology (of tissue fixed with NBF) to either confirm the clinical diagnosis or to elucidate the cellular changes in tissues and lesions that are characteristic of these pathologies.

While both MRI and histology assessments are feasible in tissues fixed by perfusion using neuroanatomy solutions (i.e., AFS and SSS), previous work has not established whether studies that use registration would be feasible and of sufficient quality in these brains. Hence, the goal of the present study was to describe the protocols that are suitable for manual linear registration of the histology sections to MRI in human brain blocks fixed with three solutions (SSS and AFS used in anatomy laboratories, and NBF used in brain banks), and to compare the robustness of the alignments in different histology stains across the fixatives as well as different staining types.

METHODS

POPULATION

We used a convenience sample of 12 human brain blocks (SSS: N=4, AFS: N=4, and NBF: N=4) from our body donation program (University of Quebec in Trois-Rivieres, UQTR), that were fixed by whole-body perfusion. The bodies are injected with 25 liters of one of the three fixatives through the right common carotid artery using a pump at 30 pounds per square inch. Prior to death, the donors consented to body donation and sharing their medical information for research or teaching purposes. This study was approved by the University's Ethic Subcommittee on Anatomical Teaching and Research (UQTR) and by the Douglas Research Centre Ethic Committee (McGill University, Montreal). The mean age at time of death was 81 years old (SD=9.65; range from 64 to 96). Female to male ratio reached 2:1. The mean post-mortem interval (PMI, i.e., delay between death and injection of the fixative solution)

was 18.6 hours (SD=8.6; range from 3 to 36). The mean processing delay (PD, i.e., delay between injection of the fixative solution and MRI scans followed by histology procedures) was 32.9 months. The donors' demographics are reported in Table 1.

MAGNETIC RESONANCE IMAGING PROTOCOL

Tissue blocks of approximately 3x3x3 cm^3 were cut from regions that were macroscopically of good quality (i.e., avoid tears that could have happened during brain extraction and during removal of the arachnoid). One block containing neocortex and subcortical WM was taken from each lobe (i.e., temporal, frontal, parietal and occipital) for each of the fixative groups. Blocks were packed in small containers filled with a high-density fluoropolymer fluid free of MRI signal (Christo-Lube, Engineered Custom Lubricants). To avoid air bubbles, the tissue blocks were packed in the container while fully immersed in a bucket filled with the fluoropolymer fluid, closing the lid while the specimen and container were fully immersed. The blocks were packed so that the flat-cut surface of the block was orientated to the top (i.e., in which the high-density fluid pushed the flat surface consistently to the top of the lid), allowing for a consistent orientation of the high-resolution plane of the MRI acquisition (0.13 x 0.13 mm). Blocks were then scanned in a 7 Tesla Bruker Biospec 70/30 animal MRI scanner at the Douglas Cerebral Imaging Centre (CIC) using a Bruker transmit-receive volume coil with an 86-mm inner diameter. Six high-resolution sequences (T1-FLASH, T2-Turbo-RARE, T1-map, T2-map, T2*map, and MP2RAGE) were acquired overnight using parameters that were described in the Douglas-Bell Canada Brain Bank Post-mortem brain imaging protocol.[34]

HISTOLOGY PROCEDURES

SECTIONING AND MOUNTING

After MRI scans were completed, the tissue blocks were rinsed in 0.1M Phosphate buffer and photographed. The blocks that were too large to fit into the vibratome (Leica VT1000S) were cut and photographed again before cutting into 40 μm sections. The flat surface of the blocks was mounted on the vibratome, allowing for sectioning in the same orientation as the high-resolution plane of the MRI (since the flat surface was lying on top of the lid while scanning, which was used to adjust the field of view for the high-resolution MRI plane, and since we opened the MRI in Display to visually validate the high-resolution plane). Sections of two different levels of the blocks (also photographed), which resulted in parallel levels to the high MRI resolution plane, were selected as followed: five sections per level (ten total) were mounted on 70 x 50 mm slides and processed with five histochemistry (HC) stains. Similarly, two consecutive sections (i.e., from the same level parallel to the high MRI resolution plane) were mounted for immunohistochemistry (IHC) with 4 different antibodies. We selected the level that showed the least amount of deformation and tears to obtain these eight sec-

Table 1. Characteristics of the specimens included in this study.

Fixative	Sex	Age	Cause of death	PMI (hours)	PD (months)	Lobe
NBF	M	74	Lung cancer	3	34	Frontal R
		85	Pulmonary oedema	12	82	Parietal R
	F	84	Sepsis	21	32	Temporal L
		89	Pneumonia	23	24	Occipital R
SSS	M	83	Cardiac arrest	20	29	Occipital R
	F	67	COPD	36	41	Parietal L
		75	Pneumonia and MS	27	47	Temporal R
		87	Pneumonia	9.5	18	Frontal L
AFS	M	91	COPD	20	15	Parietal L
	F	64	Pneumonia, dementia	15.5	39	Occipital R
		96	Breast cancer	13.5	17	Temporal L
		80	Cancer	23	17	Frontal L

NBF=Neutral-buffered formalin; SSS=Saturated-salt solution; AFS=Alcohol-formaldehyde solution; F=Female; M=Male; COPD=Chronic obstructive pulmonary disease; MS=Multiple Sclerosis; PMI=post-mortem interval; PD=Processing delay; R=Right; L=Left.

tions. One section per antibody was processed with a heat-induced antigen retrieval (AR) protocol (boiling 20 minutes in 0.01M Citrate Buffer), and the other was processed with IHC directly, to avoid the potential additional tearing and deformation caused by the heat of the AR procedure. This procedure resulted in 18 mounted sections per block.

IMMUNOHISTOCHEMISTRY

IHC was used to label the four main cell populations: neurons, using neuronal nuclei (NeuN) antibodies, astrocytes, using glial fibrillary acidic protein (GFAP) antibody, microglia, using ionized binding adaptor molecule 1 (Iba1) antibody and oligodendrocytic myelin using proteolipid protein (PLP) antibody. Procedures were followed as described in Frigon et al., 2024[10] but sections were processed mounted on the slides rather than free-floating.

HISTOCHEMISTRY STAINS

We used five HC stains to label the main brain cell populations, avoiding antibodies that require antigen configuration specificity. We used Cresyl Violet (Nissl stain, which labels neurons and glial cell bodies), Luxol Fast Blue (myelin), Prussian blue staining (Perl's stain, which labels iron deposits), Bielschowsky's silver staining (which labels axons and neurofibrillary tangles) as previously described in Frigon et al., 2024.[10] We also used Hematoxylin and Eosin (H&E) Staining Kit from Abcam (ab245880) and followed their guidelines.

IMAGING

Mounted stained sections were scanned at 40X magnification with an Olympus VS120 Slide scanner at the CIC. The images were converted from .vsi format to .nifti format and downsampled by a factor of 20 to reduce file size to facilitate the registration step using an in-house MATLAB script. The resulting images were converted to minc format to al-low the use of the Register software from the MINC Tool-Kit (McConnell Brain Imaging Centre) to perform manual registration.

REGISTRATION

The T2-TurboRARE images (voxel resolution of 0.13*0.13*0.5 mm) were used for registration with histology since they provide good anatomical contrast that are close to *in vivo* images, in comparison to post-mortem T1w images in which the gray level contrast is reversed.[34] Registration between histology images and MRIs was performed using a manual linear registration approach (3 rotations, 3 translations, 1 scale), tagging a minimum of 4 landmarks using Register software (included in the MINC Tool-Kit). More fiducial markers (i.e., tags) were placed if necessary, and the required number was considered as a variable of interest (see next section). Since all the acquired post-mortem sequences are co-registered together, histology images could also be co-registered to the other acquired sequences using the same transformations. The same approach was repeated to register the block photos to the MRIs.

VARIABLES OF INTEREST

HISTOLOGY QUALITY

STAINING INTENSITY

Histological staining intensity of the sections was qualitatively assessed as it could impact the alignment of the tissue (i.e., if certain parts of the tissue are not sufficiently stained, then those areas could be impossible to align). Darker sections were considered of higher histological quality, since they provided clearer visualization of anatomical landmarks.

Pale=0 ([Figure 1A](#)); Heterogeneous=1 ([Figure 1B](#)); Dark=2 ([Figure 1C](#)).
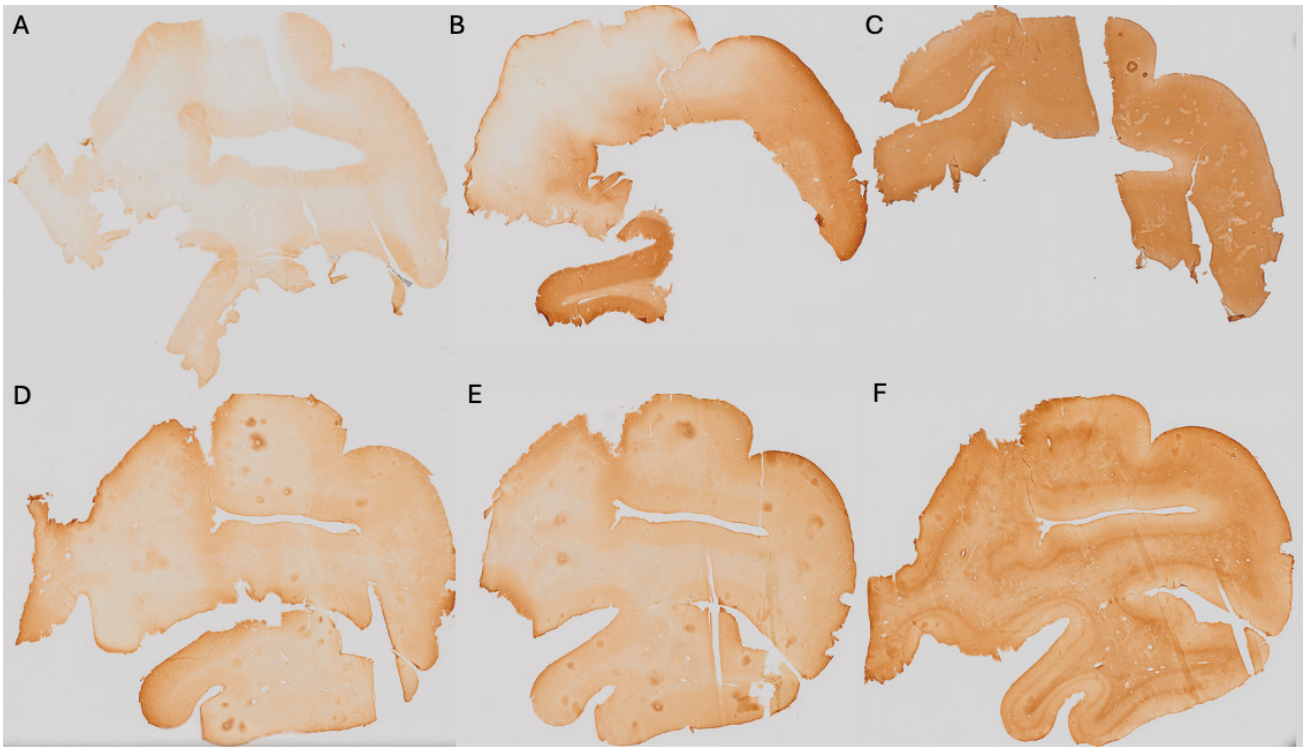
Figure 1. Criteria for assessment of the histology quality variable.

Staining intensity showing A) Pale section=0; B) Heterogeneous section=1 and C) Dark section=2. GM-WM contrast showing D) No contrast=0; E) Blurred contrast=1 and F) Sharp contrast=2. These sections come from the right occipital block fixed with SSS.

GRAY MATTER TO WHITE MATTER CONTRAST

The GM-WM contrast was assessed since more contrast on the histology sections allows for better placement of markers on different boundaries of the tissue (i.e., pial surface of the GMc and GMc-to-WM boundary). A sharp GM-WM contrast reflected higher histological quality, since it provided a clearer visualization of anatomical landmarks.

No contrast=0 (Figure 1D); Blurred contrast=1 (Figure 1E); Sharp contrast=2 (Figure 1F).

REGISTRATION QUALITY

NUMBER OF TAGS

The number of tags used for manual registration was considered a variable reflecting the ease of registration. If more than 4 tags were needed (minimum to initiate manual alignment), this suggested a more complex registration. An example of the anatomical landmarks (6 tags) that were used is shown in Figure 2.

TISSUE BLOCK-MRI-HISTOLOGY COLOCALIZATION

Using Display software from the MINC toolkit, we segmented the surfaces of the same level of the MRI slide (Figure 3A) and the photograph of the tissue block (Figure 3B) registered to the corresponding histology section (Figure 3C). The histology sections were segmented by an expert with more than 8 years of experience (EMF), creating the following masks: Label 1 (Red)=Non-folded/Non-torn tissue (Good quality); Label 2 (Green)=Folded tissue; Label

3 (Blue)=Torn tissue; and Label 4 (Cyan)=Non-folded/Non-torn tissue that was not parallel to the MRI plane (Good quality but off plane) (Figure 3C). The surface of each mask was calculated as number of pixels in the MRI image space by transforming the histology and tissue block images to the MRI image space using the generation transforms. The MRI and photo block masks (Figure 3A-B) were then overlapped (Figure 4A) to assess the amount of tissue that was cut from the scanned block to be able to fit the vibratome. Then, the overlap of the histology mask (Label 1, Non-folded/Non-Teared tissue) and the photo block mask (Figure 3B-C and Figure 4B) was used to assess the percentage of tissue loss in the histology sections. Dice Kappas of the overlapped masks were also calculated to assess the amount of overlap. All measurements were generated automatically using an in-house MATLAB script. The percentage of tissue showing Good quality was then compared according to the fixatives and the staining types. We also assessed the mean percentage of Folded tissue and Torn tissue for each group to assess if the quality of the histology section affected the registration quality.

STATISTICAL ANALYSIS

Qualitative variables (sections 'Staining intensity' and 'GM-WM contrast') were assessed using chi-square test. Quantitative variables (sections 'Number of tags and 'Tissue block-MRI-histology colocalization') were assessed using Kruskal-Wallis analyses according to their distribution. All the variables were compared between the three experimental groups (NBF, SSS and AFS), as well as between
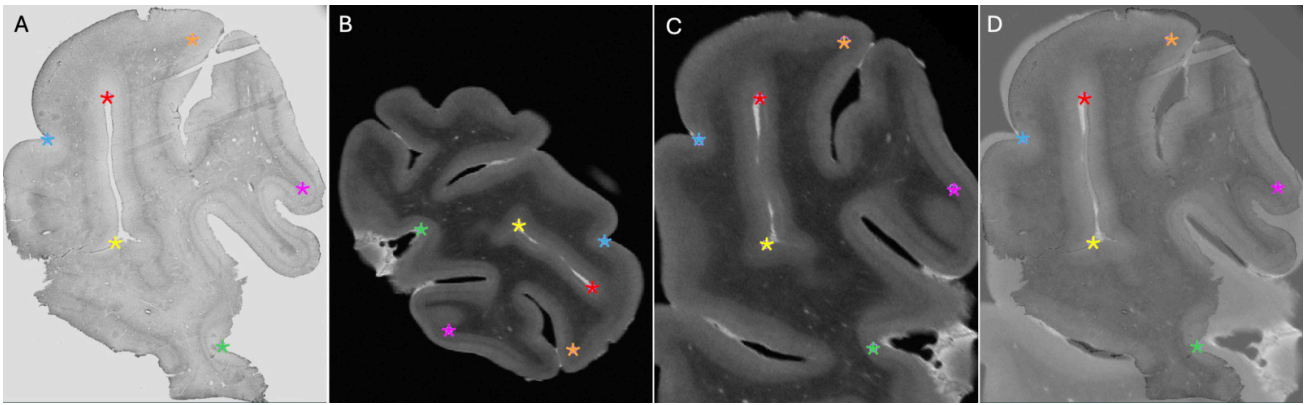
Figure 2. Process of the manual registration using landmarks.

A) Histology section. B) Native T2-TurboRARE MRI sequence. C) T2-TurboRARE MRI registered to the histology section. D) Overlap of the histology and registered MRI. Colored stars (6 tags in total: orange, red, blue, pink, yellow and green) show the landmarks that were used to initiate the registration between A and B, which resulted in C, and the overlap of both modalities in D.
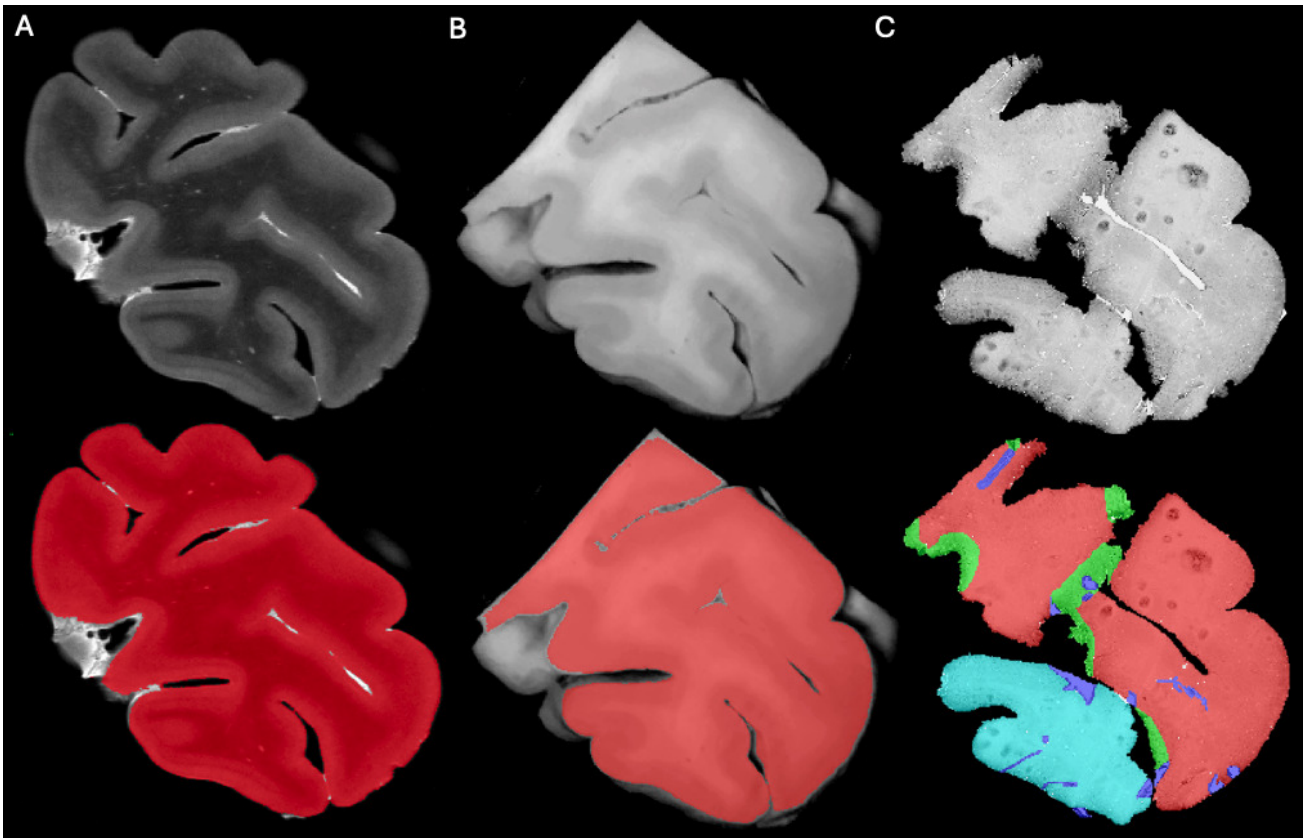

Figure 3. Masks created using Display to assess histology-MRI colocalization.

Masks were created for A) MRI slide registered to the histology section; B) Photo of the block cut to fit in the vibratome, registered to the MRI-histology section; C) Histology section photomicrographs. Red masks=Non-folded/Non-torn tissue (Good quality); Green masks=Folded tissue; Blue masks=Torn tissue; and Cyan blue= Non-folded/Non-torn tissue that was not parallel to the MRI plane (Good quality but off plane).

the three different staining types (IHC with AR, IHC without AR and HC). All variables were also assessed individually within the comparison groups so that the variables were evaluated independently. All statistical analyses were conducted using IBM SPSS statistics (version 29.0.2.0) and were adjusted for multiple comparisons following a Bonferroni correction.

RESULTS

HISTOLOGY QUALITY

STAINING INTENSITY

No significant difference was found in the staining intensity of the histology sections across the three fixatives (p=0.696)
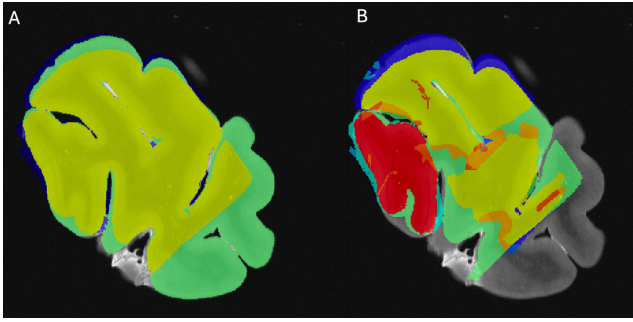
Figure 4. Overlap of the masks segmented to assess the amount of histology tissue colocalizing with MRI scans.

A) Overlap of the MRI plane and block photo masks that was considered as the target for assessment of the histology sections that co-localized. B) Overlap of the histology (with the four labels) to the block photo masks that is overlapped with the MRI picture, which was assessed according to the two groups (fixatives and type of staining).

(Figure 5, top left). However, when considered individually, in IHC sections processed with AR, SSS-fixed brains showed a significantly lower frequency of Dark sections (p=0.0037) and a higher number of Heterogeneous sections (p=0.045), while the later did not retain significance after a Bonferroni correction. The other two staining types (IHC without AR and HC) showed the same pattern as the overall staining intensity according to the fixatives (Figure 5, left column).

According to the impact of the staining types, IHC with AR showed more sections with a heterogeneous staining intensity, but this did not retain significance after a Bonferroni correction (uncorrected p=0.04). IHC without AR showed a significantly higher number of Pale sections than with AR and HC staining (p<0.0001) and significantly fewer Dark sections (p=0.0003). Finally, HC sections showed significantly fewer Pale sections (p=0.0007) and a significantly higher number of Dark sections (p<0.0001) (Figure 5, top right). When considered individually within the fixative groups, NBF, SSS and AFS brain blocks followed the same pattern of a higher number of Dark sections in HC sections, and a higher number of Pale sections while lower number of Dark sections in IHC without AR (Figure 5, third column).

GRAY MATTER TO WHITE MATTER CONTRAST

GM-WM contrast showed significant differences between sections of blocks that were fixed with the three solutions (p=0.03). NBF-fixed blocks showed fewer sections with a Blurred contrast than the other two solutions, but this did not retain significance after a Bonferroni correction (uncorrected p=0.016). SSS-fixed blocks showed a significantly higher number of Blurred contrast (p=0.005) and significantly fewer Sharp contrast (p=0.005) than the sections fixed with the other two solutions (Figure 5, top row, second column). When considered individually, sections processed with IHC without AR showed a significantly higher number of Blurred GM-WM contrast when fixed with SSS (p=0.005), and sections processed with HC also showed more sections with Blurred contrast and fewer with Sharp contrast, but this did not retain significance after Bonferroni correction

(p=0.037 and p=0.0069, respectively) (Figure 5, second column).

GM-WM contrast was also significantly affected by the staining type (p=0.001). IHC with AR did not show any statistical difference. However, IHC without AR showed significantly more sections with No contrast (p=0.0003) and fewer sections with a Sharp contrast than HC, but this did not retain significance after a Bonferroni correction (uncorrected p=0.012). Finally, HC staining showed significantly fewer sections with No contrast (p=0.0002) and more sections with Sharp contrast, but this did not retain significance after Bonferroni correction (uncorrected p=0.0069) (Figure 5, bottom right). This pattern was also observed when blocks fixed with the three fixatives were considered individually; NBF-fixed and AFS-fixed blocks processed with IHC without AR showed significantly more sections with No contrast than when processed with the other two staining types (p=0.0027 and p=0.0037, respectively) (Figure 5, fourth column).

REGISTRATION QUALITY

NUMBER OF TAGS

SSS-fixed blocks required significantly more tags to initiate alignment (median=6, range 4-16) than the blocks that were fixed with the other two solutions (NBF; median=5, range 4-25; p=0.002 and AFS, median=4, range 4-10; p<0.001) (Figure 6A). The staining type (IHC with AR, IHC without AR and HC) did not have an impact on the number of tags that were necessary to manually register the sections, since no significant difference (p=0.55) was found across groups (IHC-AR, median=6, range 4-25; IHC-noAR, median=5, range 4-9; HC, median=5, range 4-16) (Figure 6B).

TISSUE BLOCK-MRI-HISTOLOGY COLOCALIZATION

We used the overlap of the photo block and MRI (Figure 4A) as the target of the histology masks to assess the percentage of the histology sections of Good quality (label 1=Non-folded/Non-torn tissue) that colocalized with the MRIs. AFS-fixed blocks showed significantly higher overlap (%) between the MRI and Good quality histology mask (median=80.49, range 18-97, median kappa=0.892) than SSS-fixed blocks (median=67.40, range 0-93, median kappa=0.805) (p=0.012) (Figure 7 top left). Percentage of the good quality histology masks overlap with MRI and tissue block overlap were significantly different between the staining types, with a median of IHC with AR, IHC without AR and HC of 50.78 (range 0-96, median kappa=0.674), 76.45 (range 25-97, median kappa=0.841) and 72.46 (range 18-96, median kappa=0.870) respectively (p<0.001). IHC with AR histology sections showed significantly less overlap than IHC without AR (p<0.001) and HC (p=0.003) (Figure 7, top right).

We also found that there was a higher percentage of Torn tissue in the brain blocks fixed with SSS, but this did not retain significance after a Bonferroni correction (Figure 7, bottom left). The histology sections processed with IHC
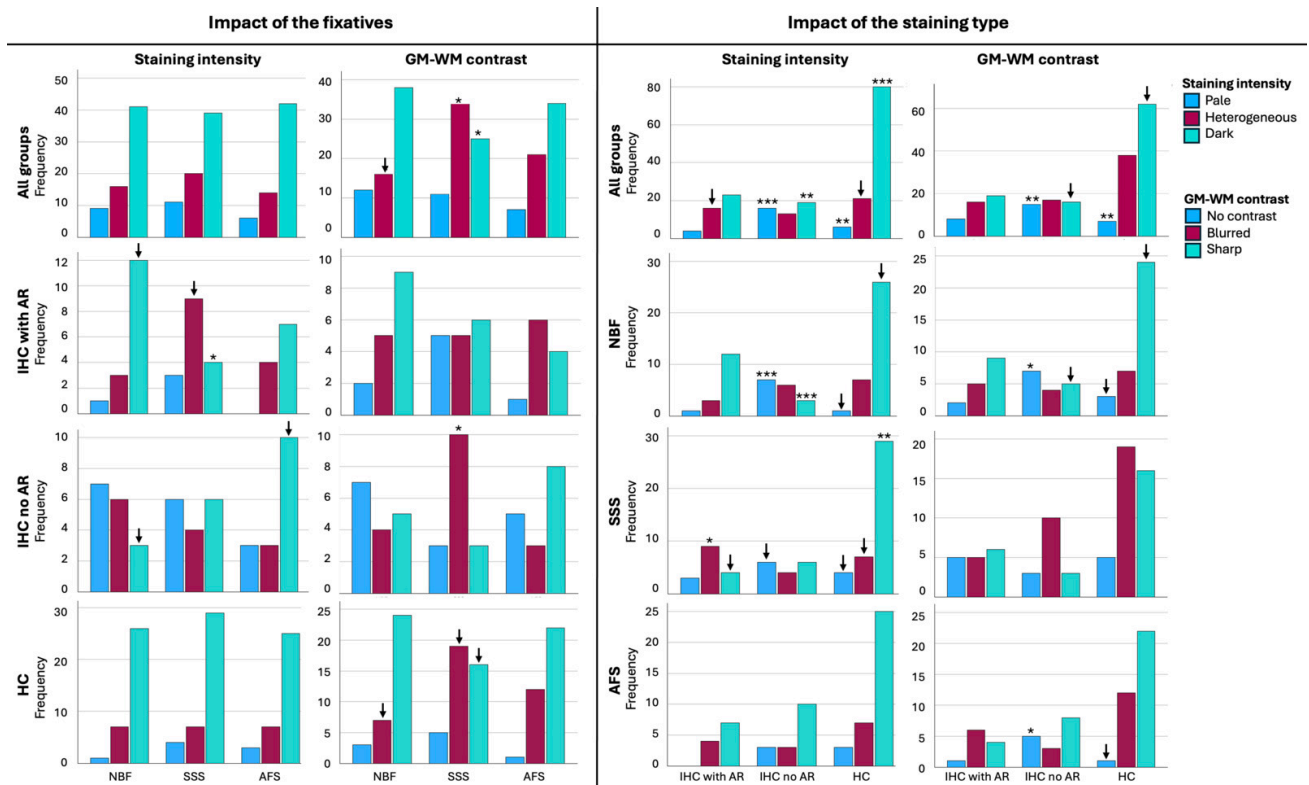
Figure 5. Histology quality of the sections regarding staining intensity and gray to white matter (GM-WM) contrast.

Left graphs show the impact of the fixatives (NBF=Neutral-buffered formalin; SSS=Saturated-salt solution; AFS=Alcohol-formaldehyde solution) on the staining intensity (left column) and GM-WM contrast (right column). Right graphs show the impact of the staining type (IHC=Immunohistochemistry; AR=Antigen retrieval; HC= Histochemistry) on the staining intensity (left column) and GM-WM contrast (right column). Top row shows the results of the histology quality when all groups were considered together. Second, third and 4th row show the results of the histology quality when the groups are assessed individually (IHC with AR, IHC without AR and HC, respectively, for the impact of the fixatives, and NBF, SSS and AFS, respectively, for the impact of the staining type). ↓p<0.05 before Bonferroni correction; *p<0.005; **p<0.001; ***p<0.0001.

without AR (median=3.24, range 0.82-23.60) showed significantly less Folded tissue than sections processed with HC (median=4.13, range 0-25.57, p=0.027) and with IHC with AR (median=5.08, range=1.35-71.40, p=0.004) ([Figure 7](#), bottom right).

DISCUSSION

This study aimed to describe the quality of linear registration between histology sections and MRI in human brain blocks fixed with three solutions, and in histology sections that were processed with different staining types to provide new insights on registration protocols of brain blocks from gross anatomy laboratories.

HISTOLOGY QUALITY

STAINING INTENSITY

Since we had previously found slight differences in the background staining intensity of mice brains fixed with SSS,[9] we assessed intensity of the background staining on a scale of pale to dark. Although we acknowledge that higher staining intensity does not always reflect good histological quality, we assessed staining intensity as it could impact the visibility of anatomical landmarks on the histology sec-

tions, consequently affecting the registration quality; it was not intended as a measure of cell preservation. In microscopic cellular assessment, an increased staining intensity would not be ideal since it hides the contrast between cells and the background. However, for registration purposes, there is a degree of staining intensity that must be dark enough to allow for landmark visualization to place the tags but also pale enough to still see the contrast with the cells for further biological analysis. Here, we found a higher frequency of Dark sections (which helps the rater placing the tags for the manual linear registration to decide on the landmarks that will be selected) in the blocks fixed with the three solutions, reflecting no impact of the chemical composition of the different solutions on the staining background when considered altogether ([Figure 5](#), top left). However, SSS-fixed brains showed a higher number of Heterogeneous sections and lower Dark sections when processed with IHC with AR, while more Pale sections were also observed when processed with IHC without AR in these cases. Therefore, staining intensity of immunohistochemistry procedures seems to be affected more in SSS samples. This is in accordance with the fact that SSS-fixed brains showed less homogeneous distribution of the antigens of interest (perhaps less staining intensity) in our previous study.[10]
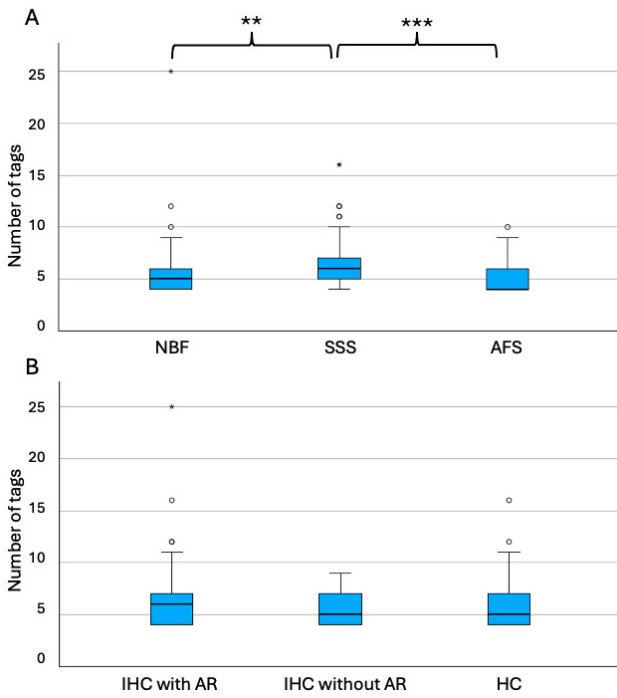
Figure 6. Number of tags necessary to register the sections

A) according to the fixative and B) according to the type of staining. NBF=Neutral-buffered formalin SSS=Saturated-salt solution; AFS=Alcohol-formaldehyde solution; IHC=Immunohistochemistry; AR=Antigen retrieval; HC=Histochemistry. **p<0.001; ***p<0.0001.

Furthermore, the staining intensity seems to be affected by the staining type. Indeed, HC showed significantly more Dark sections, which was expected as our previous assessments had also shown strong labeling and no impact of fixative.[10] Furthermore, antigenicity preservation (and therefore staining intensity) was not homogeneous between the antibodies and the fixatives.[10] Our results showed that IHC without AR have significantly more sections with both pale and dark backgrounds, especially when fixed with NBF, while IHC with AR showed more Heterogeneous sections, especially when fixed with SSS. This could be caused by the fact that AR increases antigen staining but also may decrease in some cases non-specific background labeling.[10,35-37]

GRAY MATTER TO WHITE MATTER CONTRAST

Gray to white matter contrast was also assessed since it could have an impact on the chosen landmarks and therefore on the registration quality. We found that SSS-fixed brain blocks showed a higher number of sections with Blurred contrast compared to the other solutions, especially when they were processed with IHC without an antigen retrieval protocol. This was consistent with our previous observations showing a slightly lower contrast of the MRIs in SSS-fixed brains.[12] This is also consistent with previous findings in histochemical sections where SSS-fixed brains showed paler neurons in Cresyl violet stain, heterogeneous fibers in Luxol fast blue, and lower quality in Bielschowsky's staining, as well as lower antigenicity distribution without AR.[10] GM-WM contrast was also affected by
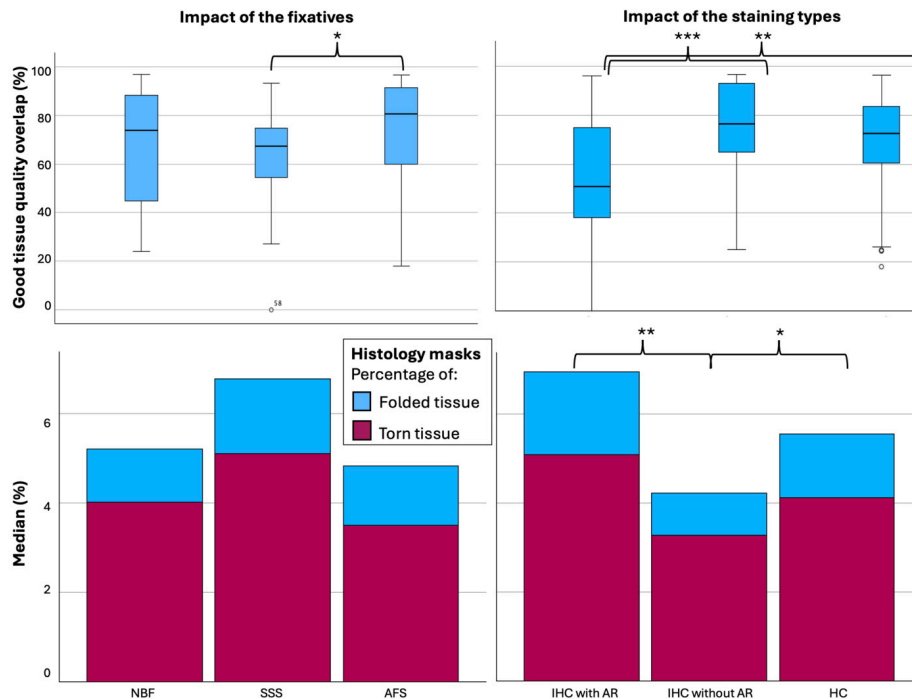

Figure 7. Tissue block-MRI-histology overlap of the masks to assess colocalization.

Left graphs show the impact of the fixative (NBF=Neutral-buffered formalin; SSS=Saturated salt solution; AFS=Alcohol-formaldehyde solution) on the percentage of the Good quality tissue overlap (top) and the Median percentage of Folded (blue) and Torn (purple) tissue (bottom). Right graphs show the impact of the staining type (IHC=Immunohistochemistry; AR=Antigen retrieval; HC= Histochemistry) on the percentage of the Good quality tissue overlap (top) and the median percentage of Folded (blue) and Torn (purple) tissue (bottom). *p<0.05; **p<0.01; ***p<0.001.

the staining type, where IHC without AR showed more sections without contrast. Again, this is because AR increases the labeling of the cells and therefore shows a higher differentiation between gray and white matter layers, otherwise this is lacking when no antigen retrieval is applied to the procedure.

REGISTRATION QUALITY

The number of tags that were used to manually register the T2-TurboRARE sequence with histology sections was significantly different in the brains fixed with the three solutions. AFS and NBF-fixed blocks required fewer tags than the SSS-fixed blocks, reflecting a more difficult registration with the latter. This is consistent with our previous findings that SSS-fixed tissue is more friable and difficult to manipulate than the other fixatives, resulting in more tears and folding of the tissue,[10] and therefore more distortions compared to the MRI sections. This is also supported by our quantitative analysis of the percentage of Good quality tissue masks, where we found that SSS-fixed blocks showed less overlap with the tissue block masks than AFS-fixed sections, and that a higher percentage of Torn tissue was found in the SSS-fixed brains. Although this latter statement did not retain statistical significance, it was again consistent with previous qualitative findings of our team.[10]

Regarding the relation between registration quality and the staining types, we found no difference in the number of tags required to initiate manual alignment between the three solutions. However, we found a higher Good tissue quality overlap and less Folded and Torn tissue in the histology sections that were processed with IHC without an antigen retrieval protocol. Indeed, we expected that it would be more difficult to register the sections when an AR protocol was conducted prior to IHC since it is known to enhance tissue tearing and tissue loss.[10,38] However, AR staining being darker (higher contrast with the cells which resulted in a higher GM-WM contrast), it was unexpectedly easy to put the tags in most cases, since it enhanced the visibility of the landmarks. Therefore, we suggest using an AR protocol in IHC even if this results in a more difficult manipulation of the sections, since it also results in a better staining and therefore, better correlates with MRI findings.

GROUPS OF COMPARISON

FIXATIVES

Immersion of freshly extracted brains in 10% NBF is a ubiquitous fixation protocol in brain banks.[8,34] This is currently coined as the control group since neuroscientific findings have been made with these brains so far. However, NBF solution is not ideal for anatomy dissection and also show inconveniences in histology and MRIs since the surface of the brain shows signs of over-fixation, while the deep white matter and nucleus is more poorly preserved.[39,40] Furthermore, brain banks offer very few and small tissue samples to researchers, so we suggest that brains from anatomy laboratories may be used as an alternative. Moreover, perfusion fixation with NBF is feasible,[41] and can be combined

with perfusing the rest of the body with another solution.[42] This would allow the adequate preparation of cadaveric specimens for gross dissection and surgical training along with optimal brain preservation for histochemical and immunohistochemical processing. However, practices in multiple anatomy laboratories are not yet ideal and use AFS and SSS as alternatives.

Our results support that AFS provides a good alternative for fixation, since it preserves brain MRI contrasts,[11,12] histology quality and manual registration of both modalities in a good manner, as well as for combining gross anatomy dissection and histology assessment of different tissues.[43-50]

Conversely, SSS-fixed brains are of lesser quality, impacting the registration of MRI and histology images, although still feasible and of sufficient quality. These brain blocks require greater care in manipulation and histology protocols to achieve registration results closer to those obtained with the other two solutions. This is probably due to the lower amount of formaldehyde in its formulation,[51] leading to a poorer preservation of the tissue integrity, as explained in our previous findings.[10]

STAINING TYPE

IHC without AR group included the 4 labeled sections per specimen (NeuN, GFAP, Iba1 and PLP) that did not go through an AR procedure, while IHC with AR did. We decided to separate these two groups since we considered that heat-induced antigen retrieval could impact: 1-GM-WM contrast and staining intensity and 2-tears and folding of the tissue as we observed in a previous study of our group.[10] Furthermore, we chose to include 4 IHC stains (NeuN, GFAP, Iba1, and PLP) to label the main brain cell populations (i.e., neurons, astrocytes, microglia and myelin), which are commonly used in histopathology diagnosis, using protocols already validated for the three solutions in our previous study, which made this new assessment more robust.[10]

The HC protocols included the two levels of sections using five different stains (i.e., ten slices per specimen), to label: 1) the endoplasmic reticulum and cellular nuclei, which stained cell bodies of neurons and glial cells, using a Cresyl Violet and a Neutral red staining[52]; 2) the myelin of oligodendrocytes using Luxol Fast Blue,[53] frequently used in multiple sclerosis, Alzheimer's disease or cerebrovascular diseases[17,24,26-28,30-32,54-56]; 3) the ferric iron aggregation in the neuropil of the brain, using a Prussian blue staining (Perl's stain),[57-59] commonly used in different white matter pathologies detected by MRI, or again, neurodegenerative diseases[28,60-64]; 4) the nerve fibers and neurofibrils using Bielschowsky's silver staining method,[65] used typically to demonstrate axonal tangles and senile plaques,[66-73] and 5) the cell bodies and small capillaries using H&E staining, the most common histopathological stain used in diagnosis of neuropathology.[26,27,29,54,61,72,74-76] HC stains seem generally more robust than IHC, giving the highest staining intensity and sharpest GM-WM contrast. This can be related to the fact that antigens and epitopes recognition, which can be modified by cross-linking of the proteins related to

chemical fixation, is not involved in these HC staining protocols.

LIMITATIONS

We acknowledge that this study was conducted with a small convenience sample. Therefore, all statistical results should be mostly considered as descriptively informative. Nonetheless, while there were only 4 blocks per fixative, this resulted in 9 stains per blocks * 12 = 120 stains and their subsequent registrations. The samples were heterogeneous in terms of the cause of death, the post-mortem delay, and the cortical area; however, we always took neocortex and subcortical WM for all the blocks. The use of this heterogeneous sample may be seen as a disadvantage by most, since the control of as many variables as possible is what is generally desired when designing an experiment. However, we consider this heterogeneity as an advantage for the general scope of our research, which is the assessment of MRI and histology feasibility in specimens of unpredictable characteristics, since we have no control on the comorbidities, causes of death, etc. of the donors that arrive to anatomy laboratories. So, this study shows that even in different circumstances and with various confounding variables, which could affect the tissue quality, registration between histology and MRI is still feasible. Finally, the small sample size resulted in heterogeneous groups of comparison regarding the staining types. It is not possible to know the impact of each antigen of interest (NeuN, GFAP, Iba1 and PLP) considered individually since they were included in the same staining type. Another limitation of this study is that our blocks were too large to be cut as they were scanned (we had to trim them to fit them in the vibratome). This resulted in an impossible direct comparison on tissue loss and colocalization between the histology and MRIs. However, we tried to overcome this issue by segmenting masks of the photographs of the tissue blocks after being trimmed, of the MRIs, and of the histology to facilitate the comparisons. Finally, we also had to deal with sections that showed Good histology results but that were off plane (Label 4 of the masks), which resulted in poor registration quality (high number of tags) since they were not cut parallel to the MRI scans (i.e., poorer orientation of the flat surface of the block on top of the lid while scanning). However, this is not a problem related to the fixative groups or the staining type, but it could have impacted the overall results. This problem could be resolved in future studies by applying an automatic nonlinear registration to the histology-MRI manual registration (Note: our in-house pipelines for automatic nonlinear registration are still under development).

CONCLUSION

We conclude that brain blocks fixed with solutions used in gross anatomy laboratories, preferably an AFS, may be used for manual linear registration of histology photomicrographs and high-resolution MRIs of the blocks, allowing to take advantage of the two most common neuroimaging modalities. This is promising for neuroscientists interested in using larger brain samples from anatomy laboratories to correlate histology findings with MRI and possibly increase knowledge on biomarkers of normal aging or neurodegenerative disease in post-mortem diagnosis.

CONFLICTS OF INTEREST

The authors report no competing interests

REFERENCES

1. Feczko E, Augustinack JC, Fischl B, Dickerson BC. An MRI-based method for measuring volume, thickness and surface area of entorhinal, perirhinal, and posterior parahippocampal cortex. *Neurobiol Aging*. 2009;30(3):420-431. doi:10.1016/j.neurobiolaging.2007.07.023

2. Apostolova LG, Zarow C, Biado K, et al. Relationship between hippocampal atrophy and neuropathology markers: a 7T MRI validation study of the EADC-ADNI Harmonized Hippocampal Segmentation Protocol. *Alzheimers Dement*. 2015;11(2):139-150. doi:10.1016/j.jalz.2015.01.001

3. Meyer CR, Moffat BA, Kuszpit KK, et al. A methodology for registration of a histological slide and in vivo MRI volume based on optimizing mutual information. *Mol Imaging*. 2006;5(1):16-23.

4. Dadar M, Mahmoud S, Zhernovaia M, Camicioli R, Maranzano J, Duchesne S. White matter hyperintensity distribution differences in aging and neurodegenerative disease cohorts. *Neuroimage Clin*. 2022;36:103204. doi:10.1016/j.nicl.2022.103204

5. Cardoso JR, Pereira LM, Iversen MD, Ramos AL. What is gold standard and what is ground truth? *Dental Press J Orthod*. 2014;19(5):27-30. doi:10.1590/2176-9451.19.5.027-030.ebo

6. Hoffmann A, Bredno J, Wendland MF, et al. Validation of in vivo magnetic resonance imaging blood-brain barrier permeability measurements by comparison with gold standard histology. *Stroke*. 2011;42(7):2054-2060. doi:10.1161/strokeaha.110.597997

7. Carlos AF, Poloni TE, Medici V, Chikhladze M, Guaita A, Ceroni M. From brain collections to modern brain banks: A historical perspective. *Alzheimers Dement (N Y)*. 2019;5:52-60. doi:10.1016/j.trci.2018.12.002

8. Vonsattel JP, Amaya M del P, Cortes EP, Mancevska K, Keller CE. Twenty-first century brain banking: practical prerequisites and lessons from the past: the experience of New York Brain Bank, Taub Institute, Columbia University. *Cell Tissue Bank*. 2008;9(3):247-258. doi:10.1007/s10561-008-9079-y

9. Frigon EM, Dadar M, Boire D, Maranzano J. Antigenicity is preserved with fixative solutions used in human gross anatomy: A mice brain immunohistochemistry study. *Front Neuroanat*. Published online October 12, 2022:16. doi:10.3389/fnana.2022.957358

10. Frigon EM, Gérin-Lajoie A, Dadar M, Boire D, Maranzano J. Comparison of histological procedures and antigenicity of human post-mortem brains fixed with solutions used in gross anatomy laboratories. *Front Neuroanat*. 2024;18:1372953. doi:10.3389/fnana.2024.1372953

11. Frigon EM, Pharand P, Gérin-Lajoie A, et al. T1- and T2-weighted MRI signal and histology findings in suboptimally fixed human brains. *J Neurosci Methods*. 2024;412:110301. doi:10.1016/j.jneumeth.2024.110301

12. Maranzano J, Dadar M, Bertrand-Grenier A, et al. A novel ex vivo, in situ method to study the human brain through MRI and histology. *J Neurosci Methods*. 2020;345:108903. doi:10.1016/j.jneumeth.2020.108903

13. Choe AS, Gao Y, Li X, Compton KB, Stepniewska I, Anderson AW. Accuracy of image registration between MRI and light microscopy in the ex vivo brain. *Magnetic Resonance Imaging*. 2011;29(5):683-692. doi:10.1016/j.mri.2011.02.022

14. Goubran M, de Ribaupierre S, Hammond RR, et al. Registration of in-vivo to ex-vivo MRI of surgically resected specimens: a pipeline for histology to in-vivo registration. *J Neurosci Methods*. 2015;241:53-65. doi:10.1016/j.jneumeth.2014.12.005

15. Singh M, Rajagopalan A, Kim TS, et al. Co-registration of In-Vivo Human MRI Brain Images to Postmortem Histological Microscopic Images. *Int J Imaging Syst Technol*. 2008;18(5-6):325-335. doi:10.1002/ima.v18:5/6

16. Bobinski M, de Leon MJ, Wegiel J, et al. The histological validation of post mortem magnetic resonance imaging-determined hippocampal volume in Alzheimer's disease. *Neuroscience*. 2000;95(3):721-725. doi:10.1016/s0306-4522(99)00476-5

17. Bronge L, Bogdanovic N, Wahlund LO. Postmortem MRI and histopathology of white matter changes in Alzheimer brains. A quantitative, comparative study. *Dement Geriatr Cogn Disord*. 2002;13(4):205-212. doi:10.1159/000057698

18. Frigerio I, Boon BDC, Lin CP, et al. Amyloid-β, p-tau and reactive microglia are pathological correlates of MRI cortical atrophy in Alzheimer's disease. *Brain Commun*. 2021;3(4):fcab281. doi:10.1093/braincomms/fcab281

19. Goubran M, Crukley C, de Ribaupierre S, Peters TM, Khan AR. Image registration of ex-vivo MRI to sparsely sectioned histology of hippocampal and neocortical temporal lobe specimens. *Neuroimage*. 2013;83:770-781. doi:10.1016/j.neuroimage.2013.07.053

20. Mega MS, Chen SS, Thompson PM, et al. Mapping histology to metabolism: coregistration of stained whole-brain sections to premortem PET in Alzheimer's disease. *Neuroimage*. 1997;5(2):147-153. doi:10.1006/nimg.1996.0255

21. Scheltens P, Barkhof F, Leys D, Wolters EC, Ravid R, Kamphorst W. Histopathologic correlates of white matter changes on MRI in Alzheimer's disease and normal aging. *Neurology*. 1995;45(5):883-888. doi:10.1212/wnl.45.5.883

22. Pozorski V, Oh JM, Adluru N, et al. Longitudinal white matter microstructural change in Parkinson's disease. *Hum Brain Mapp*. 2018;39(10):4150-4161. doi:10.1002/hbm.24239

23. Stille M, Smith EJ, Crum WR, Modo M. 3D reconstruction of 2D fluorescence histology images and registration with in vivo MR images: application in a rodent stroke model. *J Neurosci Methods*. 2013;219(1):27-40. doi:10.1016/j.jneumeth.2013.06.003

24. Gouw AA, Seewann A, van der Flier WM, et al. Heterogeneity of small vessel disease: a systematic review of MRI and histopathology correlations. *J Neurol Neurosurg Psychiatry*. 2011;82(2):126-135. doi:10.1136/jnnp.2009.204685

25. Grinberg LT, Amaro Junior E, da Silva AV, et al. Improved detection of incipient vascular changes by a biotechnological platform combining post mortem MRI in situ with neuropathology. *J Neurol Sci*. 2009;283(1-2):2-8. doi:10.1016/j.jns.2009.02.327

26. Humphreys CA, Jansen MA, Muñoz Maniega S, et al. A protocol for precise comparisons of small vessel disease lesions between ex vivo magnetic resonance imaging and histopathology. *Int J Stroke*. 2019;14(3):310-320. doi:10.1177/1747493018799962

27. Lahna D, Roese N, Woltjer R, et al. Postmortem 7T MRI for guided histopathology and evaluation of cerebrovascular disease. *J Neuropathol Exp Neurol*. 2022;82(1):57-70. doi:10.1093/jnen/nlac103

28. Roseborough AD, Langdon KD, Hammond R, et al. Post-mortem 7 Tesla MRI detection of white matter hyperintensities: A multidisciplinary voxel-wise comparison of imaging and histological correlates. *NeuroImage: Clinical*. 2020;27:102340. doi:10.1016/j.nicl.2020.102340

29. Solé-Guardia G, Custers E, de Lange A, et al. Association between hypertension and neurovascular inflammation in both normal-appearing white matter and white matter hyperintensities. *Acta Neuropathol Commun*. 2023;11(1):2. doi:10.1186/s40478-022-01497-3

30. Filippi M, Brück W, Chard D, et al. Association between pathological and MRI findings in multiple sclerosis. *Lancet Neurol*. 2019;18(2):198-210. doi:10.1016/s1474-4422(18)30451-4

31. Laule C, Kozlowski P, Leung E, Li DK, Mackay AL, Moore GR. Myelin water imaging of multiple sclerosis at 7 T: correlations with histopathology. *Neuroimage*. 2008;40(4):1575-1580. doi:10.1016/j.neuroimage.2007.12.008

32. Laule C, Moore GRW. Myelin water imaging to detect demyelination and remyelination and its validation in pathology. *Brain Pathol*. 2018;28(5):750-764. doi:10.1111/bpa.12645

33. Moll NM, Rietsch AM, Thomas S, et al. Multiple sclerosis normal-appearing white matter: pathology-imaging correlations. *Ann Neurol*. 2011;70(5):764-773. doi:10.1002/ana.22521

34. Dadar M, Sanches LG, Fouquet J, et al. The Douglas-Bell Canada Brain Bank Post-mortem Brain Imaging Protocol. *Apuerture Neuro*. 2024;4. doi:10.52294/001c.123347

35. Krenacs L, Krenacs T, Stelkovics E, Raffeld M. Heat-induced antigen retrieval for immunohistochemical reactions in routinely processed paraffin sections. *Methods Mol Biol*. 2010;588:103-119. doi:10.1007/978-1-59745-324-0_14

36. Shi SR, Liu C, Pootrakul L, et al. Evaluation of the value of frozen tissue section used as "gold standard" for immunohistochemistry. *Am J Clin Pathol*. 2008;129(3):358-366. doi:10.1309/7cxuyxt23e5al8kq

37. Shi SR, Shi Y, Taylor CR. Antigen retrieval immunohistochemistry: review and future prospects in research and diagnosis over two decades. *J Histochem Cytochem*. 2011;59(1):13-32. doi:10.1369/jhc.2010.957191

38. Evers P, Uylings HB, Suurmeijer AJ. Antigen retrieval in formaldehyde-fixed human brain tissue. *Methods*. 1998;15(2):133-140. doi:10.1006/meth.1998.0616

39. Garman RH. Artifacts in routinely immersion fixed nervous tissue. *Toxicol Pathol*. 1990;18(1 Pt 2):149-153. doi:10.1177/019262339001800120

40. Beach TG, Tago H, Nagai T, Kimura H, McGeer PL, McGeer EG. Perfusion-fixation of the human brain for immunohistochemistry: comparison with immersion-fixation. *J Neurosci Methods*. 1987;19(3):183-192. doi:10.1016/s0165-0270(87)80001-8

41. McFadden WC, Walsh H, Richter F, et al. Perfusion fixation in brain banking: a systematic review. *Acta Neuropathol Commun*. 2019;7(1):146. doi:10.1186/s40478-019-0799-y

42. Insausti R, Insausti AM, Muñoz López M, et al. Ex vivo, in situ perfusion protocol for human brain fixation compatible with microscopy, MRI techniques, and anatomical studies. *Front Neuroanat*. Published online March 23, 2023:17. doi:10.3389/fnana.2023.1149674

43. Venne G, Zec ML, Welte L, Noel G. Qualitative and quantitative comparison of Thiel and phenol-based soft-embalmed cadavers for surgery training. *Anat Histol Embryol*. 2020;49(3):372-381. doi:10.1111/ahe.12539

44. Tomalty D, Pang SC, Ellis RE. Preservation of neural tissue with a formaldehyde-free phenol-based embalming protocol. *Clin Anat*. 2019;32(2):224-230. doi:10.1002/ca.23290

45. Rahman SMN, Alam T, Alam NN. Preservation of Histology by Phenol-Based Fixative: Mini Review of Recent Findings. *International Journal of Morphology*. 2021;39:50-56.

46. O'Sullivan E, Mitchell BS. An improved composition for embalming fluid to preserve cadavers for anatomy teaching in the United Kingdom. *J Anat*. 1993;182(Pt 2):295-297.

47. Martins-Costa C, Nunes TC, Anjos-Ramos LD. Anatomo-comparative study of formaldehyde, alcohol, and saturated salt solution as fixatives in Wistar rat brains. *Anat Histol Embryol*. 2022;51(6):740-745. doi:10.1111/ahe.12852

48. Hopwood D, Slidders W, Yeaman GR. Tissue fixation with phenol-formaldehyde for routine histopathology. *Histochem J*. 1989;21(4):228-234. doi:10.1007/bf01747525

49. Benet A, Rincon-Torroella J, Lawton MT, González Sánchez JJ. Novel embalming solution for neurosurgical simulation in cadavers. *J Neurosurg*. 2014;120(5):1229-1237. doi:10.3171/2014.1.Jns131857

50. Barton DP, Davies DC, Mahadevan V, et al. Dissection of soft-preserved cadavers in the training of gynaecological oncologists: report of the first UK workshop. *Gynecol Oncol*. 2009;113(3):352-356. doi:10.1016/j.ygyno.2009.02.012

51. Coleman R, Kogan I. An improved low-formaldehyde embalming fluid to preserve cadavers for anatomy teaching. *J Anat*. 1998;192(Pt 3):443-446. doi:10.1046/j.1469-7580.1998.19230443.x

52. Eilam-Altstädter R, Las L, Witter MP, Ulanovsky N. Methods. In: Eilam-Altstädter R, Las L, Witter MP, Ulanovsky N, eds. *Stereotaxic Brain Atlas of the Egyptian Fruit Bat*. Academic Press; 2021:1-9. doi:10.1016/B978-0-12-819297-9.00001-5

53. Lindberg MR, Lamps LW. Central Nervous System. In: Lindberg MR, Lamps LW, eds. *Diagnostic Pathology: Normal Histology*. 2nd ed. Elsevier; 2018:108-111. doi:10.1016/B978-0-323-54803-8.50029-2

54. Li K, Rashid T, Li J, et al. Postmortem Brain Imaging in Alzheimer's Disease and Related Dementias: The South Texas Alzheimer's Disease Research Center Repository. *J Alzheimers Dis*. 2023;96(3):1267-1283. doi:10.3233/jad-230389

55. Kuhlmann T, Ludwin S, Prat A, Antel J, Brück W, Lassmann H. An updated histological classification system for multiple sclerosis lesions. *Acta Neuropathol*. 2017;133(1):13-24. doi:10.1007/s00401-016-1653-y

56. Ouellette R, Mangeat G, Polyak I, et al. Validation of Rapid Magnetic Resonance Myelin Imaging in Multiple Sclerosis. *Ann Neurol*. 2020;87(5):710-724. doi:10.1002/ana.25705

57. Churukian CJ. 14 - Pigments and Minerals. In: Bancroft JD, Gamble M, eds. *Theory and Practice of Histological Techniques*. 6th ed. Churchill Livingstone; 2008:233-259. doi:10.1016/B978-0-443-10279-0.50021-X

58. Guindi M. 11 - Liver Disease in Iron Overload. In: Saxena R, ed. *Practical Hepatic Pathology: A Diagnostic Approach*. 2nd ed. Elsevier; 2018:151-165. doi:10.1016/B978-0-323-42873-6.00011-1

59. Xiao G, Li H, Zhao M, Zhou B. Chapter Eight - Assessing metal ion transporting activity of ZIPs: Intracellular zinc and iron detection. In: Hu J, ed. *Methods in Enzymology*. Academic Press; 2023:157-184. doi:10.1016/bs.mie.2023.05.011

60. Connor JR, Benkovic SA. Iron regulation in the brain: histochemical, biochemical, and molecular considerations. *Ann Neurol*. 1992;32 Suppl:S51-61. doi:10.1002/ana.410320710

61. Kruer MC. The neuropathology of neurodegeneration with brain iron accumulation. *Int Rev Neurobiol*. 2013;110:165-194. doi:10.1016/b978-0-12-410502-7.00009-0

62. Dusek P, Hofer T, Alexander J, Roos PM, Aaseth JO. Cerebral Iron Deposition in Neurodegeneration. *Biomolecules*. 2022;12(5). doi:10.3390/biom12050714

63. Stüber C, Morawski M, Schäfer A, et al. Myelin and iron concentration in the human brain: a quantitative study of MRI contrast. *Neuroimage*. 2014;93 Pt 1:95-106. doi:10.1016/j.neuroimage.2014.02.026

64. van Duijn S, Nabuurs RJ, van Duinen SG, Natté R. Comparison of histological techniques to visualize iron in paraffin-embedded brain tissue of patients with Alzheimer's disease. *J Histochem Cytochem*. 2013;61(11):785-792. doi:10.1369/0022155413501325

65. Ogawa Y. Silver Impregnation Method for Neurons Using Synthetic Surfactants: A Contribution to Golgi Method. In: Conn PM, ed. *Quantitative and Qualitative Microscopy*. Methods in Neurosciences; 1990. doi:10.1016/B978-0-12-185255-9.50024-9

66. Stahnisch FW. Max Bielschowsky (1869-1940). *J Neurol*. 2015;262(3):792-794. doi:10.1007/s00415-014-7544-z

67. Wisniewski HM, Wen GY, Kim KS. Comparison of four staining methods on the detection of neuritic plaques. *Acta Neuropathol*. 1989;78(1):22-27. doi:10.1007/bf00687398

68. Love S, Nicoll JA. Comparison of modified Bielschowsky silver impregnation and anti-ubiquitin immunostaining of cortical and nigral Lewy bodies. *Neuropathol Appl Neurobiol*. 1992;18(6):585-592. doi:10.1111/j.1365-2990.1992.tb00830.x

69. Allsop D. Introduction to Alzheimer's disease. *Methods Mol Med*. 2000;32:1-21. doi:10.1385/1-59259-195-7:1

70. Switzer RC 3rd. Application of silver degeneration stains for neurotoxicity testing. *Toxicol Pathol*. 2000;28(1):70-83. doi:10.1177/019262330002800109

71. Uchihara T. Silver diagnosis in neuropathology: principles, practice and revised interpretation. *Acta Neuropathol*. 2007;113(5):483-499. doi:10.1007/s00401-007-0200-2

72. Kovacs GG, Budka H. Current concepts of neuropathological diagnostics in practice: neurodegenerative diseases. *Clin Neuropathol*. 2010;29(5):271-288. doi:10.5414/npp29271

73. Elobeid A, Rantakömi S, Soininen H, Alafuzoff I. Alzheimer's disease-related plaques in nondemented subjects. *Alzheimers Dement*. 2014;10(5):522-529. doi:10.1016/j.jalz.2012.12.009

74. Vakrakou AG, Brinia ME, Svolaki I, Argyrakos T, Stefanis L, Kilidireas C. Immunopathology of Tumefactive Demyelinating Lesions-From Idiopathic to Drug-Related Cases. *Front Neurol*. 2022;13:868525. doi:10.3389/fneur.2022.868525

75. Beach TG, Sue LI, Scott S, et al. Cerebral white matter rarefaction has both neurodegenerative and vascular causes and may primarily be a distal axonopathy. *J Neuropathol Exp Neurol*. 2023;82(6):457-466. doi:10.1093/jnen/nlad026

76. Fischer AH, Jacobson KA, Rose J, Zeller R. Hematoxylin and eosin staining of tissue and cell sections. *CSH Protoc*. 2008;2008:pdb.prot4986. doi:10.1101/pdb.prot4986

SUPPLEMENTARY MATERIALS

Supplementary material

Download: https://apertureneuro.org/article/154293-histology-to-mri-registration-quality-of-ex-vivo-human-brain-blocks-fixed-with-solutions-used-in-anatomy-laboratories/attachment/322715.docx